Nanophase Segregation and Water Dynamics in the Dendrion Diblock Copolymer Formed from the Fréchet Polyaryl Ethereal Dendrimer and Linear PTFE

Seung Soon Jang, Shiang-Tai Lin, Tahir Çağın, Valeria Molinero, and William A. Goddard III*

Materials and Process Simulation Center (MC 139-74), California Institute of Technology, Pasadena, California 91125

Received: January 7, 2005; In Final Form: March 31, 2005

We propose a new material consisting of a dendrion copolymer formed from (a) a water-soluble dendritic polymer and (b) a hydrophobic backbone. Using molecular dynamics simulations techniques, we determine the structure and dynamics of the dendrion formed by second-generation Fréchet polyaryl ethereal dendrimer as the hydrophilic component and linear polytetrafluoroethylene (PTFE) as the hydrophobic polymer, with 5 and 10 wt % of water. We find that this material produces a well-developed nanoscale structure in which water forms a continuous nanophase, making this new family of compounds promising candidates for applications in fuel cell membranes. We find that the water molecules are incorporated into the dendrimer block of the copolymer to form a nanophase-segregated structure. The well-developed nanophase-segregated structures rendered by this material have characteristic dimensions of segregation (∼30 Å) and dendrimer conformational properties that are independent of water content. Calculations of water dynamics and proton transport in these nanophase-segregated structures indicate that the dendrion copolymer membrane with 10 wt % of water content has a water structure and transport properties equivalent to that of the hydrated Nafion membrane with 20 wt % of water content.

1. Introduction

Since the concept of a polymer electrolyte membrane fuel cell (PEMFC) was introduced as an alternative electrical power source in 1960, enormous efforts have been devoted to developing such practical applications as all-electric automobiles.[1−4] The state of the art for current PEMFC technologies utilizes hydrated perfluorosulfonic (PFS) polymers such as Nafion, which exhibits high proton conductivity (0.1 S/cm at 30 °C with ∼21−22 H_2O/SO_3^-) as well as excellent chemical and thermal stability up to nearly 170 °C.[5−9] Despite successes, there remain problems with Nafion-based PEMFC. Thus, it is desirable to operate fuel cells at above 120 °C to prevent poisoning of the Pt catalysts by CO, but for temperatures above 100 °C, the Nafion-based systems lose water, leading to poor proton conductivity. Consequently, there is great interest in finding replacements for Nafion that could operate at higher temperatures while retaining the high proton conductivity and other favorable properties of Nafion.

A general consensus from experiments[2,10−24] and simulations[25−27] is that an important factor in the favorable properties of PFS-polymer-based PEMFC is its nanophase-segregated structure, which consists of a hydrophobic phase of perfluorinated polymer backbone interspersed with a hydrophilic water phase associated with the sulfonic groups of the polymer. In previous studies,[28] we showed that the characteristic dimensions of the nanophase-segregated structure can be controlled by the specific monomeric sequence of the Nafion polymer, which in turn controls the transport characteristics of PEMFC. Thus, we found[28] that Nafion polymers with identical chemical compositions but different distributions of sulfonic acid groups along the polymer chain lead to dramatically different phase segregation in the membranes, which in turn results in dramatic changes in the transport properties.

On the basis of these insights about the origins of the favorable properties of Nafion for PEMFC, we concluded that it might be possible to improve the performance of PEMFC by combining dendritic polymers providing a regular distribution of acid sites with a simple hydrophobic backbone such as PTFE. Favorable factors motivating the consideration of dendrimers are as follows:

1. The well-defined regular structure arising from a monodisperse molecular-weight distribution achievable by the stepwise iterative synthetic route.

2. The availability of numerous terminal groups at the periphery (or surface) of the dendrimer, which increases exponentially with the generation (and molecular weight).

Thus, we expect to control the solubility and mechanical properties dominated by these terminal groups by controlling the generation number of the appropriate dendrimer. Indeed, such aspects of dendrimers have been investigated extensively for applications ranging from rheological modifiers to drug (or gene) delivery and light-harvesting (or light-emitting) nanotechnology.[29−31] Our focus here is to utilize these well-controllable features of dendrimers to manipulate the nanophase segregation of the dendrion, which aims at optimizing its performance in PEMFCs. As a proof of concept, we present here the specific case of a *dendrion hybrid copolymer* based on the second-generation water-soluble polyaryl ethereal Fréchet dendrimer,[32] shown in Figure 1: each dendrimer has sixteen carboxylic acid moieties connected to a biphenyl core through aryl ether units (carboxylic dendrion). We also present similar studies of the sulfonic acid version of the dendrion copolymer

* To whom correspondence should be addressed. wag@wag.caltech.edu.

10.1021/jp050125w CCC: $30.25
Published on Web 04/27/2005

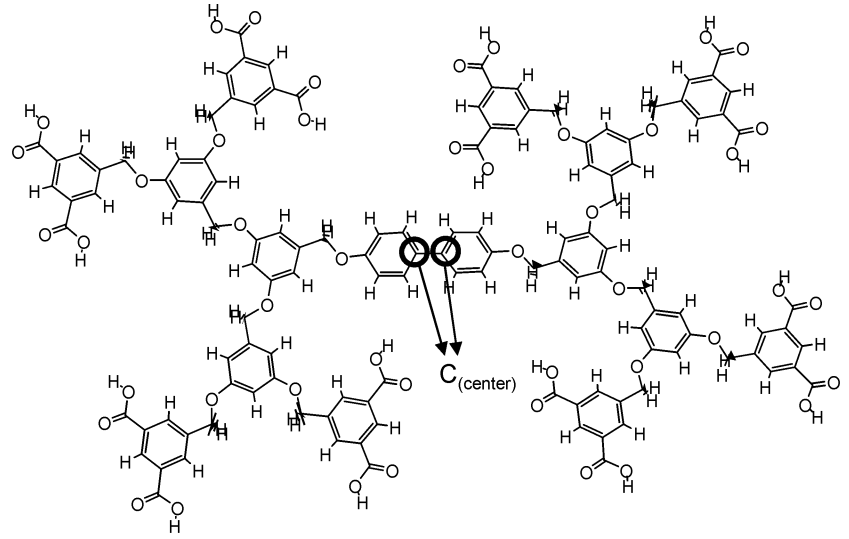

(a) carboxylic dendrimer

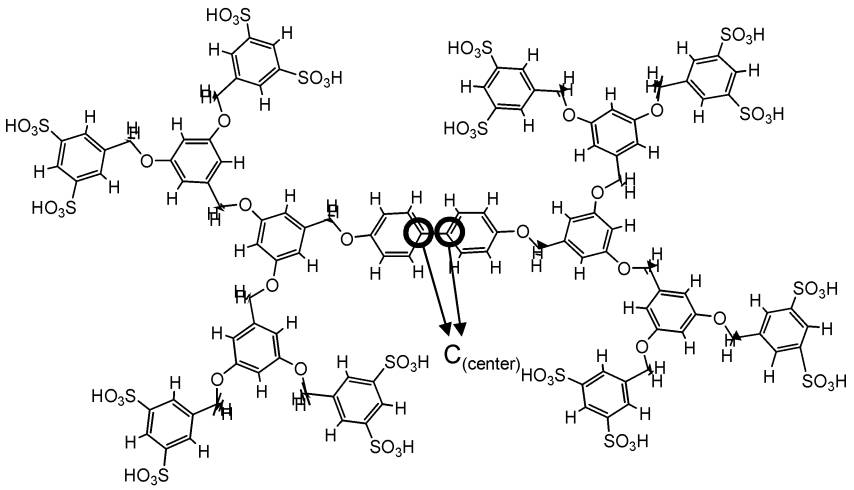

(b) sulfonic dendrimer

Figure 1. Chemical structure of the second-generation water-soluble polyaryl ethereal dendrimer (Fréchet dendrimer[32]). This has sixteen acid groups, all in the terminal generation. The carbons marked $C_{(center)}$ are used as the central carbons for the analysis in Figure 10. (a) Chemical structure of the dendrion consisting of a second-generation Fréchet dendrimer linked to linear PTFE diblock copolymer. (b) Fully extended atomistic model of the second-generation Fréchet dendrimer−linear PTFE diblock copolymer: left, carboxylic dendrion; right, sulfonic dendrion.

(sulfonic dendrion) to estimate the effect of the dendrion architecture on proton transport.

For the hydrophobic backbone of the dendrion (covalently connected to the dendrimer), we consider here linear polytetrafluoroethylene (PTFE). There have been a few studies on the synthesis and properties in solution or at the air/solvent interface of such hybrid architectures,[33−44] but there remain many questions about the condensed-phase properties of this interesting architecture.

We expected that the hybrid molecular architecture (Figure 1) of the dendrion would lead to a nanophase-segregated structure in which hydrophilic dendrimers are incorporated with solvent (water in this study) to form solvent clusters and channels. This has been observed in the diblock copolymers of linear polystyrene and acid-functionalized poly(propylene imine) dendrimer, where Román et al.[45] used small-angle X-ray scattering and transmission electron microscopy to investigate its microphase separation. Without a covalent connection between hydrophilic dendrimer and hydrophobic PTFE backbone, we expect that phas segregation would take place over macroscopic scales, which is not desirable for PEMFC applications, because water management in systems exhibiting large phase-segregation would be difficult, and poor entanglement between dendrimers would result in poor mechanical stability. In this paper, we choose to use a simple PTFE backbone, because we are most concerned with the properties of the dendrimer. However, it is plausible that such a PTFE backbone would tend to crystallize, leading to phase separation from the hydrophilic dendrimer block. Thus, we consider that it would be better to control the crystallizability of the backbone by cross-linking the hydrophobic backbone as in Nafion or by increasing the flexibility of the PTFE backbone with small amounts of comonomers (C_2H_4, $CHFCF_2$, CH_2CF_2, $CFClCF_2$, etc.) during the polymerization step. This might improve the mechanical and transport properties of the membrane while retaining the proton transport properties and the stability in strong acids. We plan to study some such modifications later.

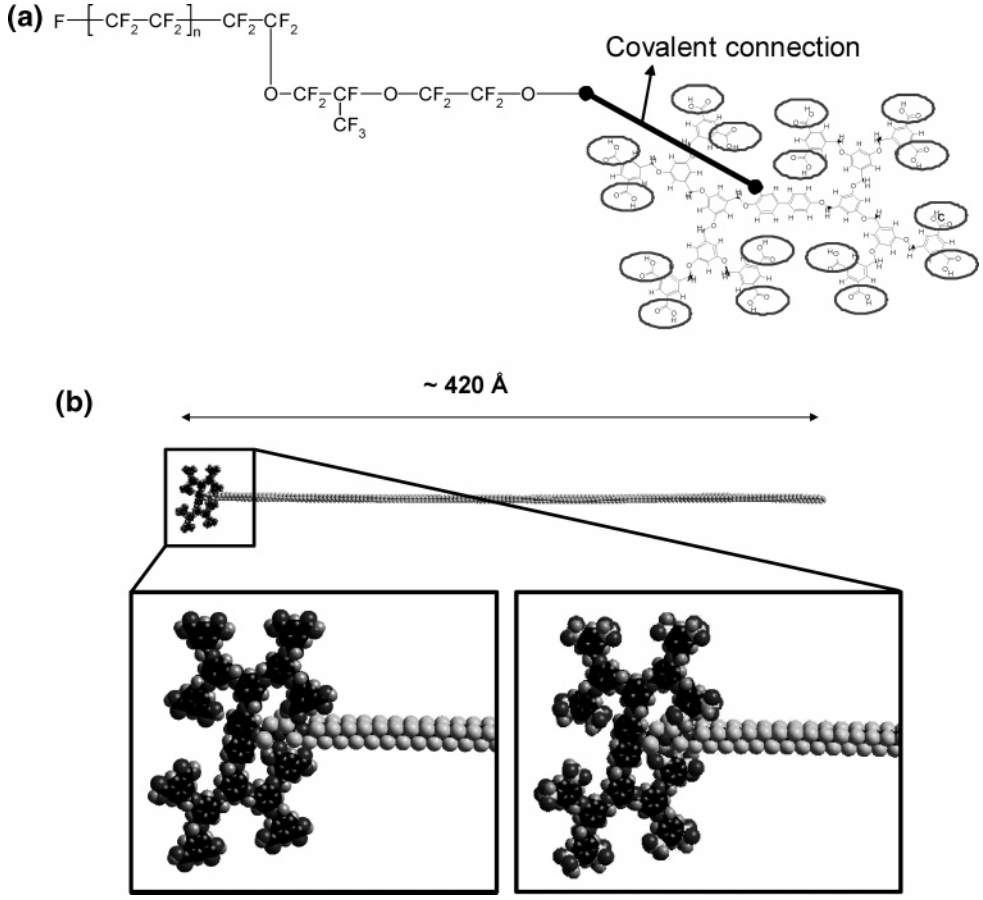

Figure 2. Chemical and geometric structures of the dendrion. The degree of polymerization (*n*) is 149, corresponding to an equivalent weight of 1102.

Because such polar groups as carboxylic and sulfonic acid are localized at the periphery of the dendrimer, we expected that the dendritic architecture would lead to a well-defined spatial distribution of the polar groups in membranes. We also expected that the nanophase-segregated structure and transport properties of water in the membrane can be controlled systematically by changing such variables as dendrimer generation, acid group moieties, equivalent weight of the copolymer, and water content.

In this study, we use molecular dynamics (MD) simulations to obtain detailed information about the structural and dynamical properties of the Fréchet dendrimer−PTFE dendrion. The use of atomistic MD simulation methods is most appropriate for studying new PEMFC, because we can determine its nanophase-segregated structure without a bias toward any specific model. These studies determine how the nanostructure depends on such variables as water content, temperature, and molecular architecture of the polymer. Here, we focus mainly on the water content at a given molecular architecture in order to determine how the water molecules are distributed in the nanophase-segregated structure of the membrane as a function of water content. Such information is critical to the performance of PEMFC, because the proton conduction occurs only through the water channel in this system.

Using the isobaric−isothermal ensemble (NPT) MD simulations, we predict the structure of the dendrion consisting of second-generation Fréchet dendrimer−linear PTFE diblock copolymers with 5 or 10 wt % of water content, and we characterize its nanophase-segregation and transport properties. The results for these dendrion systems are compared with the properties of hydrated Nafion membrane studied previously with the same methods.[28]

2. Simulation Details

All simulations were carried out using a full atomistic model of the second-generation Fréchet dendrimer−linear PTFE diblock copolymer. The degree of polymerization of the linear PTFE backbone (*n* in Figure 2) is 149, and the number of acid groups in the dendrimer is 16, so the equivalent weight of this copolymer is 1100. There are numerous ways to tie together these two dissimilar architectures, but we expect that the properties of the copolymer are relatively insensitive to the particular choice of chemical linkage. To provide this covalent connection of dendrimer to PTFE, we used the same perfluoroether linkage as in the side-chain moiety of Nafion.

2.1. Force Field. We used the Dreiding force field[46] (previously used by us[28] and others[27,47−49] to study hydrated Nafion systems), except that the fluorocarbon parts were described using recently improved force field[50] parameters and the water was described using the F3C force field.[51] We used the standard Dreiding geometric combination rules for the off-diagonal van der Waals terms. These force field parameters are described in the original papers[46,50,51] and in our previous study[28] on hydrated Nafion. Thus, the force field has the form

$$E_{\text{total}} = E_{\text{vdW}} + E_Q + E_{\text{bond}} + E_{\text{angle}} + E_{\text{torsion}} + E_{\text{inversion}} \quad (1)$$

where E_{total}, E_{vdW}, E_Q, E_{bond}, E_{angle}, E_{torsion}, and $E_{\text{inversion}}$ are the total energies and the van der Waals, electrostatic, bond

TABLE 1: Density of the Hydrated Membrane and Radius of Gyration of the Dendrimer Block

system		density (g/cm^3)		R_g (Å)	
		small system	large system	small system	large system
carboxyl dendrion	5 wt % water content	1.67 ± 0.01	1.66 ± 0.01	11.06 ± 0.07	11.09 ± 0.07
	10 wt % water content	1.61 ± 0.01	1.60 ± 0.01	11.12 ± 0.11	11.13 ± 0.08
sulfonic dendrion	10 wt % water content	1.60 ± 0.01	1.60 ± 0.01	11.02 ± 0.09	11.05 ± 0.07
dry gas phase[a]	carboxyl dendrion			11.89 ± 0.08[a]	
	sulfonic dendrion			11.73 ± 0.07[a]	

[a] From NVT MD simulation at 353.15 K for 1 ns of only the isolated second-generation Fréchet dendrimer block without the linear PTFE backbone part in gas phase. This was done for two cases and averaged.

stretching, angle bending, torsion, and inversion components, respectively.

The individual atomic charges of the copolymer were assigned using the charge equilibration (QEq) method whose parameters was optimized to reproduce Mulliken charges.[52] The atomic charges of the water molecule were from the F3C water model.[51] The Particle−Particle Particle−Mesh (PPPM) method[53] was used to calculate the electrostatic interactions.

2.2. Molecular Dynamics. All the annealing and MD simulations were performed using the MD code LAMMPS (large-scale atomic/molecular massively parallel simulator) from Plimpton at Sandia[54,55] with modifications to handle our force fields.[28,56] The equations of motion were integrated using the Verlet algorithm[57] with a time step of 1.0 fs. The Nose−Hoover temperature thermostat for the NVT and NPT calculations used the damping relaxation time of 0.1 ps and the dimensionless cell mass factor 0f 1.0.

2.3. The Simulation Cells. We constructed dendrion systems using two water concentrations: For the 10 wt % water content case, we considered both for the carboxylic dendrion and the sulfonic dendrion systems, while for the 5 wt % water content, we considered only the carboxylic dendrion system.

1. The 10 wt % case contains 4 identical diblock copolymer chains and 448 water molecules (totals of 6080 atoms for the carboxylic dendrion and 6144 atoms for the sulfonic dendrion), corresponding to an average of 7 water molecules per each acid group.

2. The 5 wt % case for the carboxylic dendrion contains the same amount of copolymer chains and 192 water molecules (5312 atoms), corresponding to 3 water molecules per acid group.

To provide a measure of the statistical uncertainties, all data in this paper were obtained from two independent samples for each amount of water using different initial configurations. We think that the two independent samples may not be sufficient to obtain accurate thermodynamic quantities such as free energy. However, the point of this paper is to determine whether a new polymer would have the appropriate water distribution in the nanophase-segregated structure for fuel cell applications. Indeed, the values reported in Tables 1, 2, and 3 indicate that such structural properties as density and radius of gyration (Table 1) are very similar for both independent samples, and furthermore, the eight times larger systems prepared independently also show very similar values. This indicates that our sampling is sufficient for our purposes, allowing the conclusions that the phase segregation and transport properties are interesting and worthy of experiments.

We expect the sulfonate groups in Nafion to be completely ionized in the presence of water (even at ∼3 wt % or 5 water per sulfonate[28]), and we expect all of the 64 sulfonate groups in the sulfonic dendrion membrane to be ionized. However, because the pK_a of carboxylic acid is ∼5 in bulk water, we expect that, for the carboxylate dendrion, the 64 carboxylic acid groups in the unit cell will not all be ionized. One could argue that none are ionized, because to have 1 deprotonated carboxylic acid group out of the 64 in our finite unit cell would imply pK_a $= -\log(1/63) = 1.8$. Consequently, we treated all carboxylates in the dendrion as neutral. Currently, we are developing methods to monitor the ionization/deionization behavior dynamically in MD simulation to provide more realistic descriptions of such systems.

In addition to the simulations described above, which use ∼5000−6000 atoms per simulation cell, we carried out independent simulations on systems eight times larger to investigate the characteristic dimension of phase segregation and to analyze characteristic dimensions. These larger scale calculations used (1) 32 identical diblock copolymer chains and 3744 water molecules in the simulation cell for 10 wt % water content (in total, 48 640 atoms for the carboxylic dendrion and 49 152 atoms for the sulfonic dendrion), corresponding to an average of 7 water molecules per each carboxylic acid group, and (2) 32 identical diblock copolymer chains and 1536 water molecules in the simulation cell for 5 wt % water content (in total, 42 496 atoms) corresponding to an average of 3 water molecules per acid group.

However, the dynamical properties (e.g., diffusion) reported here are based on the smaller system.

2.4. Construction of the Amorphous Polymer Structures. *2.4.1. The Initial Build.* The initial three-dimensional amorphous structure of each dendrion membrane was built with periodic boundary conditions using Monte Carlo techniques (the Amorphous Builder of *Cerius*^{2}[58]). In this procedure, the van der Waals radii were reduced by 70% to avoid significant unfavorable repulsive interaction between atoms. Our initial estimate for the density was 1.8 g/cm^3, on the basis of the typical density value of the hydrated amorphous phase of Nafion (no experiments have been reported on the dendrion copolymer).

2.4.2. Annealing Equilibration. The structures built with the amorphous builder can be far from equilibrium, and hence, we must anneal this starting structure to obtain an equilibrated structure expected to mimic a segment of the real amorphous system. We do this with the annealing equilibration procedure used in our previous study of Nafion.[28] This annealing procedure consists of an extensive series of simulations involving systematic variations of the volume and the temperature to achieve a fully equilibrated system at the target temperature and pressure. We emphasize here that we do *not* bias the predicted structure by imposing any particular geometry (cylinders, spheres, lamellae) for the distribution of water in the system, nor do we impose any particular density or packing. Rather, our strategy of temperature and pressure MD annealing is designed to obtain an equilibrated distribution of water in an equilibrated polymer system at target conditions (in this case, 353.15 K and 1 atm). The annealing equilibration procedure used here was as follows:

1. First, the initial cell was gradually expanded by 50% of its initial density over a period of 50 ps, while the temperature

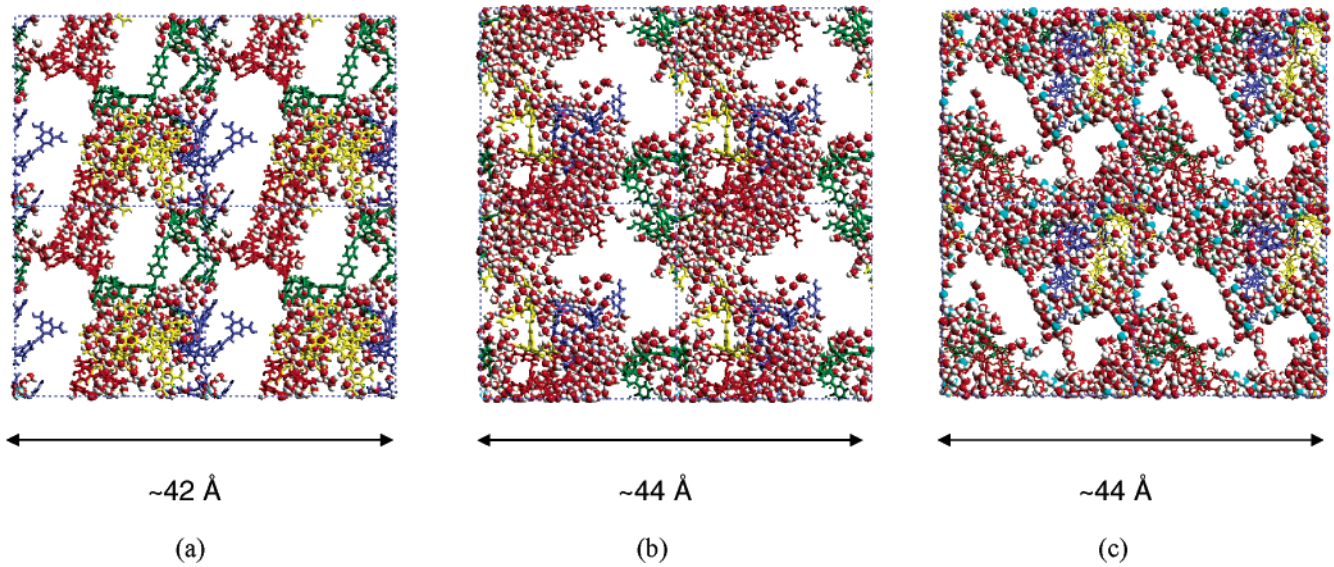

Figure 3. Nanophase-segregated structures of the dendrion membrane predicted from the simulations at 353.15 K. For clear view, the dendrimer is displayed using different color, and the PTFE chains are not shown. (a) Carboxyl dendrion with 10 wt % water, (b) carboxyl dendrion with 5 wt % water content, and (c) sulfonic dendrion with 10 wt % water.

was simultaneously increased from 300 to 600 K. Next, 50 ps of NVT MD simulations were performed at 600 K with the expanded volume.

2. Then, the structure was compressed back to the initial volume over 50 ps while cooling the temperature down to the target temperature ($T = 300$ K).

3. This expansion−compression cycle was then repeated five times.

4. Then, at the final target density (1.8 g/cm^3), we carried out 100 ps of NVT MD (fixed volume and Nose−Hoover thermostat[59] at 300K).

5. This was followed by 5 ns NPT MD at 1 atm to fully equilibrate the density and structure at the target temperature (353.15 K).

This led to a final density of 1.61 ± 0.01 g/cm^3 for the carboxylic dendrion and 1.60 ± 0.01 g/cm^3 for the sulfonic dendrion in the case of 10 wt % water content and 1.67 ± 0.01 g/cm^3 for the carboxylic dendrion in the case of 5 wt % water content. After annealing the structures as described above, we performed equilibrium NPT MD simulations for another 5 ns at 353.15 K for use in calculating properties. This is the operating temperature of Nafion-based PEMFC, which was used in previous simulations, allowing us to compare the properties of the dendrion copolymer directly with those of Nafion. We used the trajectory file for this full 5-ns NPT calculation to calculate such properties as density and pair correlation functions.

It should be noted here that this procedure was designed to yield well-equilibrated structures for complex polymers with a minimum of effort. This procedure is the same as that used in our previous study of Nafion,[28] where the objective was also to determine the extent of nanophase segregation. The main points in the annealing procedure are to impose a sequence of external temperature and volume fluctuation on the system designed to (1) help the simulated system efficiently escape from any initial local minimum in which it may have started and (2) promote the migration of species required for optimum phase segregation.

We did not calculate the changes of detailed thermodynamic properties during these annealing procedures. However, we found that the resultant structures were essentially the same even with annealing cycles greater than the five times used in our current study. Thus, we believe that our procedure is sufficient to prepare the system for our purpose even though it is not a unique way.

3. The Nanophase-Segregated Structure of the Dendrion

Figure 3 presents a snapshot of the final frame from the NPT MD simulations. This shows that the dendrion has a well-developed nanophase-segregated structure for both water contents. These nanophase-segregated structures show that water molecules are associated with the Fréchet dendrimer, as expected from its hydrophilic molecular character.

As summarized in Table 1, the density from the 5-ns equilibrium NPT MD simulation at 353.15 K is 1.61 ± 0.01 g/cm^3 and 1.67 ± 0.01 g/cm^3 for the carboxylic dendrion system with 10 wt % and 5 wt % water content, respectively, and 1.60 ± 0.01 g/cm^3 for the sulfonic dendrion system with 10 wt % water content. These compare well with the values obtained for the single simulation on the larger system of 1.60 ± 0.01 g/cm^3 for 10% water and 1.66 ± 0.01 g/cm^3 for 5%.

There is no experimental reference for comparison, but these density values are very comparable with the densities (1.55−1.62 g/cm^3) for hydrated Nafion membrane in our previous study.[28] This is reasonable, because the system consists mainly of perfluorinated polymer with a small amount of water.

3.1. The Fréchet Dendrimer Block. *3.1.1. The Radius of Gyration.* To obtain a reference point on the likely size of the Fréchet dendrimer block, we carried out gas-phase MD simulations (353.15 K for 1 ns) on just the dendrimer block without the linear PTFE backbone part. This led to radii of gyration (R_g) of 11.89 ± 0.08 Å for the carboxylic dendrimer and 11.73 ± 0.07 Å for the sulfonic dendrimer. Then, we analyzed the dendrions (Table 1), where we find $R_g = 11.12 \pm 0.11$ Å and 11.06 ± 0.07 Å for the carboxylic dendrion with 10 and 5 wt % water content, respectively, and $R_g = 11.02 \pm 0.09$ Å for the sulfonic dendrion with 10 wt % water content. This shows that the size of the Fréchet dendrimer is rather rigid and insensitive to the nature of the environment, decreasing by only 6% in going from the gas phase to the dendrion. Similar rigidity in dendrimers has been observed experimentally for poly(amido amine) (PAMAM) and poly(benzyl ether) dendrimers where the size of the dendrimer measured by small-angle neutron scattering

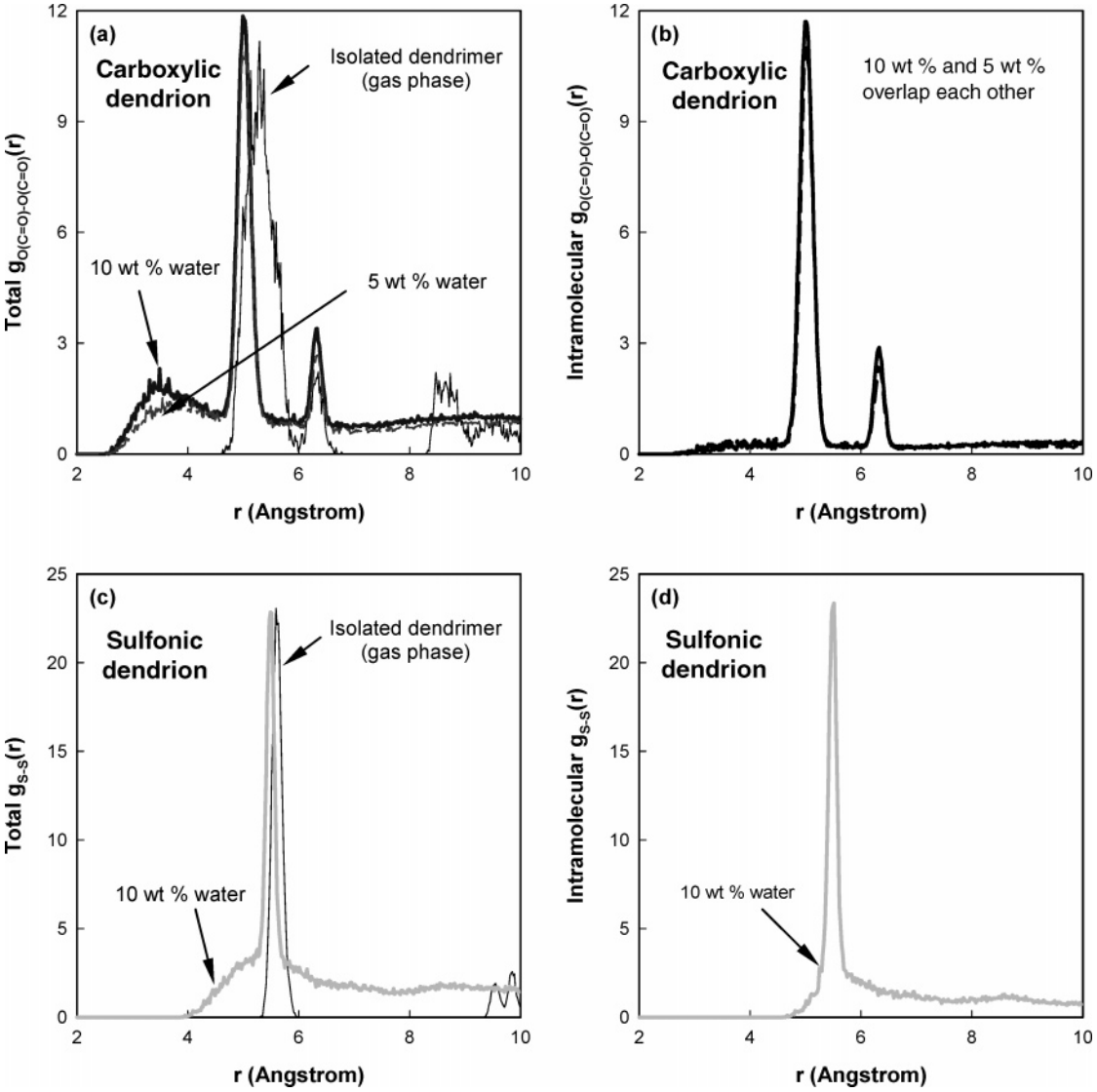

Figure 4. Pair correlation function of acid group in dendrion: For the carboxylic dendrion, the pair correlation of carbonyl oxygen−carbonyl oxygen, $g_{O(C=O)-O(C=O)}(r)$ was calculated (a) from total pairs of carbonyl oxygen−carbonyl oxygen in hydrated membrane with 10 and 5 wt % of water content at 353.15 K (also shown is the result for the isolated second-generation Fréchet dendrimer) and (b) from the pairs belonging to the same dendrimer. For the sulfonic dendrion, the pair correlation of sulfonic sulfur−sulfonic sulfur, $g_{S-S}(r)$ was calculated with 10 wt % water content.

(SANS) remains nearly constant as the solvent is changed from a poor to a good solvent.[60,61] This seems to be related to the uniform space-filling feature of the PAMAM dendrimer we observed from our previous study.[62] This insensitivity is due to the converging architecture of the dendrimer that restricts the degrees of freedom for conformational changes.

3.1.2. Correlations of the Acid Group. Figure 4 shows the pair correlation function for carbonyl oxygen−carbonyl oxygen pairs, $g_{O(C=O)-O(C=O)}(r)$, and for sulfonic sulfur-sulfonic sulfur pairs, $g_{S-S}(r)$. This pair correlation function, $g_{A-B}(r)$, indicates the probability density of finding A and B atoms at a distance r, averaged over the equilibrium trajectory as in eq 2

$$g_{A-B}(r) = \frac{\left(\frac{n_B}{4\pi r^2\, dr}\right)}{\left(\frac{N_B}{V}\right)} \qquad (2)$$

where n_B is the number of B particles located at the distance r in a shell of thickness dr from particle A, N_B is the number of B particles in the system, and V is the total volume of the system. The $g_{O(C=O)-O(C=O)}(r)$ shown in Figure 4a takes into account all the pairs of carbonyl oxygens in the system. The peaks at 5.01 and 6.30 Å correspond to the distances between pairs of carbonyl oxygens belonging to the same benzene ring (see Figure 5a). Similarly, the $g_{S-S}(r)$ in Figure 4c shows a strong peak at 5.51 Å.

First, we observe that the $g_{O(C=O)-O(C=O)}(r)$ for the intra-benzene pairs at 5.01 Å in the hydrated carboxylic dendrion membrane is 5.30 Å in the gas-phase simulation, indicating that hydration in the condensed phase brings the carbonyl oxygens closer. This is the same for the hydrated sulfonic dendrion membrane in which the peak at 5.60 Å is downshifted to that at 5.51 Å. In addition, Figure 4a shows that $g_{O(C=O)-O(C=O)}(r)$ of the hydrated membrane is affected very little by the water content. These results show that the size of the dendrimer and the spatial distribution of the carboxylic acid group are not significantly affected by the water content, which suggests that the nanophase segregation of this dendrimer−linear block is dominated by the characteristics of the molecular architecture.

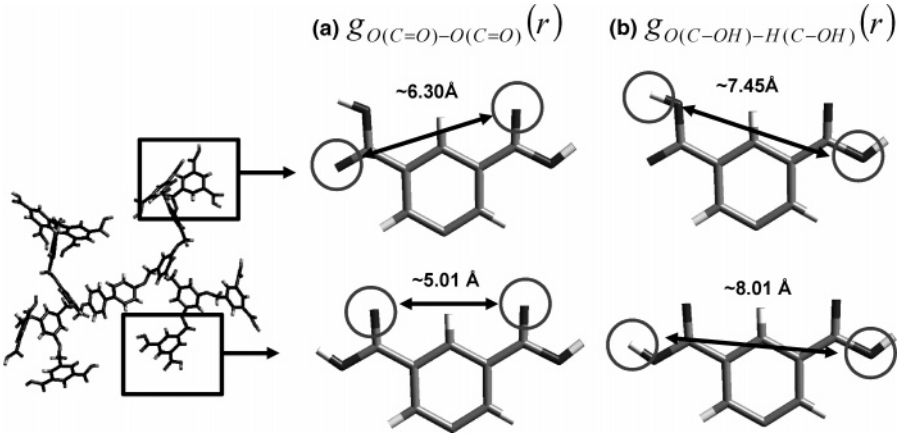

Figure 5. Diagram indicating typical distance (a) between carbonyl oxygens belonging to the same benzene, (b) between carboxyl oxygen and carboxyl hydrogen belonging to the same benzene for the second-generation Fréchet dendrimer (from gas-phase simulations at 353.15 K).

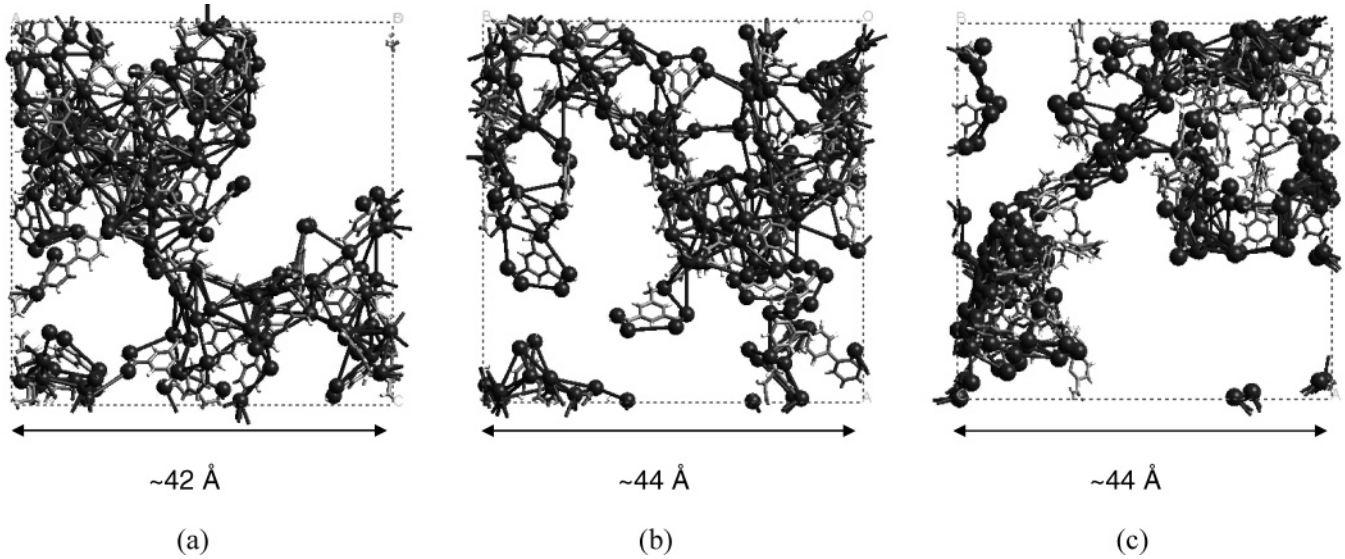

Figure 6. Distribution of oxygens in carboxylic or sulfonic acid. The bonds are generated between oxygen atoms within 7 Å. (a) Carboxylic dendrion with 10 wt % water content, (b) carboxylic dendrion with 5 wt % water content, and (c) sulfonic dendrion with 10 wt % water content.

One additional observation from Figure 4a,c is the broad small peak in the range ~2.0−5.0 Å for both water contents (10 vs 5 wt %) in the carboxylic dendrion system and ~4.0−5.0 Å for 10 wt % water content in the sulfonic dendrion system. This peak corresponds to pairs of acid groups, each of which belongs to a different dendrimer. Thus, such pair correlation at this relatively close distance is due to the contact *between* dendrimer blocks in the membrane. This is confirmed in Figure 4b,d, which shows only the intramolecular component of those pair correlation functions, where we see no peak in the above-mentioned range. This shows that the dendrimers contact each other in the hydrated membrane. This implies that the dendrion architecture has the potential to form a percolated structure of nanophase segregation, which we consider to be essential for good proton conduction. In the dendrion, the dendrimer blocks contact each other so that water molecules or protons can flow via the water phase built on this continuous dendrimer block nanophase. To clarify this point, we made bonds between oxygen atoms in (carboxylic or sulfonic) acids within 7 Å distance apart from each other, as shown in Figure 6, and thus obtained a well-interconnected oxygen lump for both water contents, which clearly indicates that *dendrimer blocks contact each other to form a percolated structure*.

3.2. The Structure Around the Waters. The characteristics of the water phase in the hydrated membrane are most important, because the proton transfer occurs in the water phase. Extensive studies on the proton transfer in water[63−72] and in polymer electrolyte membranes[3,65−67,73−75] have led to the general consensus that the proton diffusion rate in bulk water is approximately four times larger than in the hydrated membrane. As summarized by Kreuer[65,67] and by Paddison,[3] this is attributed to bulk water having a well-organized and compact hydrogen-bonding network that aids efficient proton hopping, whereas the hydrated membranes have a reduced hydrogen bond connectivity.

To characterize the structure of water in hydrated membrane, we calculated $\rho g_{O(water)-O(water)}(r)$ (see Figure 7). For comparison, the cases of bulk water and the results of our previous Nafion studies with two kinds of monomeric sequences are also presented here. We calculate a coordination number for water in the bulk water phase of 4.59, in very good agreement with the value of 4.5 computed from neutron diffraction experiments.[76] For the carboxylic dendrion membrane, we find an average water coordination number for water of 3.8 for the 10 wt % and 2.9 for the 5 wt % water content. In the sulfonic dendrion membrane, it is 3.4. These values are comparable with the value of ~3.8 for MD simulations on ionized hydrated Nafion with 20 wt % water content. Thus, we conclude that the dendrion with just half the water content reaches an

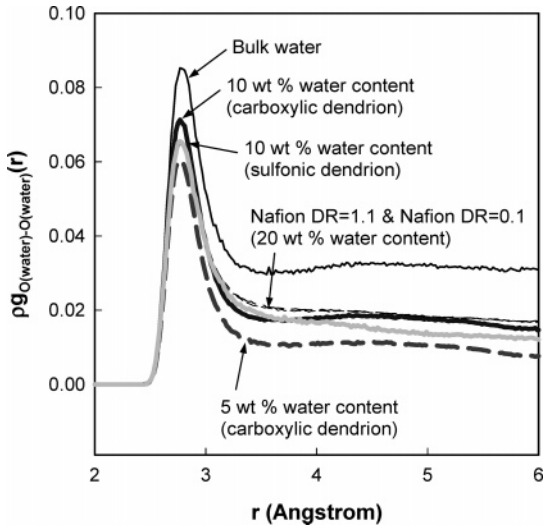

Figure 7. Product of pair correlation functions of water oxygens $g_{O(water)-O(water)}(r)$ with water number density (ρ). The dendrion reaches the same level of water structure with half the water content as the hydrated Nafion membrane.

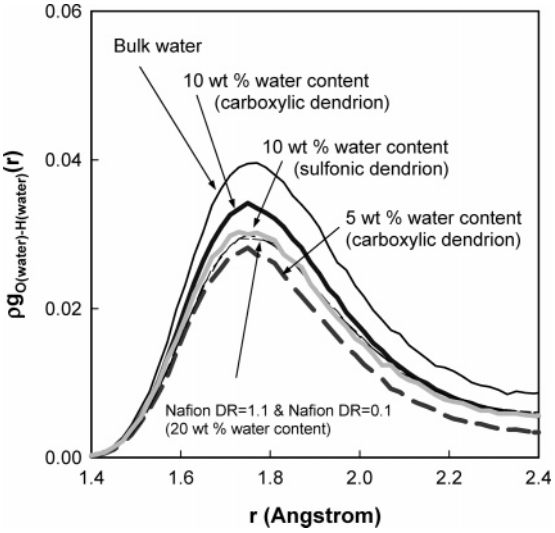

Figure 8. Product of pair correlation functions of water oxygen and water hydrogen $g_{O(water)-H(water)}(r)$ with water number density (ρ). The dendrion reaches the same level of water structure with half the water content as the hydrated Nafion membrane.

equivalent level of water structure as the hydrated Nafion membrane.

This conclusion is confirmed through $\rho g_{O(water)-H(water)}(r)$ (see Figure 8), which shows the intermolecular distance between the oxygen of water and the hydrogen of other waters in the first solvation shell. We find that the dendrion with 10 wt % water content has a similar (in sulfonic dendrion) or even larger (in carboxylic dendrion) population of bulklike intermolecular O−H distances than the Nafion-based membrane with 20% water or dendrion with 5 wt % water content. (The value obtained for bulk water here of 1.77 Å is slightly smaller than the experimental value of ∼1.80−1.85 Å,[76−78] which is a known deviation for the F3C water model.[51]) These results suggest that the water phase in the dendrion membrane can achieve the bulklike water structure more efficiently than Nafion. We had only meant by this statement that the near-neighbor distributions are similar. This water phase is well-connected to percolate through the hydrophilic dendrimer block, while simultaneously remaining well-segregated from the hydrophobic PTFE phase.

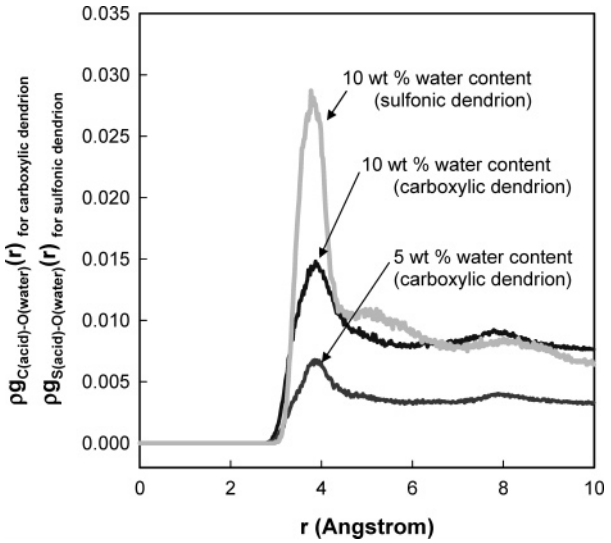

Figure 9. Product of pair correlation functions of carbon in carboxylic acid group (or sulfur in sulfonic acid group) and oxygen in water, $g_{C(acid)-O(water)}(r)$ ($g_{S(acid)-O(water)}(r)$) with water number density (ρ). The numbers of waters in the first solvation shell of the carboxylic groups are 7.3 and 3.1 for the 10 and 5 wt % water content, respectively, and that of the sulfonic acid group is 4.4 for the 10 wt % water content.

Of course, other properties, such as diffusion, are expected to be different that in bulk water.

The reason for this difference in the nanophase segregation between hydrated Nafion and hydrated dendrion is that the hydrophilic water domain in Nafion is formed only by isolated hydrophilic sulfonic acid groups. Thus, water molecules must gather separately to solvate each sulfonic acid group, leading to a structure of the water phase that is affected by the strong interaction between the ionized acid group and the water. In contrast, the dendrion has the internal space of the dendrimer in which to keep water in addition to the region nearby the hydrophilic acid group. The hydrophobicity of the internal benzyl ether moieties of the dendrimer is less than that of PTFE. Thus, after the polar groups in the periphery of the dendrimer are solvated by water, the extra water molecules should prefer this internal space of dendrimer. Because the interaction between water and the benzyl ether is somewhat weak, the water phase inside the dendrimer can form a bulklike water structure more efficiently than the water in hydrated Nafion. The rigid geometry of the dendrimer cannot change upon ionization of the acidic groups, suggesting that the structure of water in a dendrion with equivalent architecture and easily ionizable acid groups will be similar to this nonionized system, which is what we find.

3.3. The Structure Near each Acid and Inside the Dendrimer. Next, to analyze the solvation of acid groups by water, we calculated the pair correlation functions between the carbon in the carboxylic acid group and the oxygen in water, $g_{C(acid)-O(water)}(r)$, and between the sulfur in the sulfonic acid group and the oxygen in water, $g_{S(acid)-O(water)}(r)$, and their product with the water number density ρ. On the basis of Figure 9, we consider that the first solvation shell of the carboxylic acid extends to 6.0 Å. Thus, we computed the average number of water molecules surrounding each carboxylic acid group as the integral of the first peak of $\rho g_{C(acid)-O(water)}(r)$ up to 6.0 Å. Integrating this peak, we find that the number of waters in the first solvation shell of the carboxylic groups are 7.3 and 3.1 for the 10 and 5 wt % water content, respectively. In contrast, the first solvation shell of the sulfonic acid is shown up to just 4.5 Å, and the number of waters in the first solvation shell is 4.4

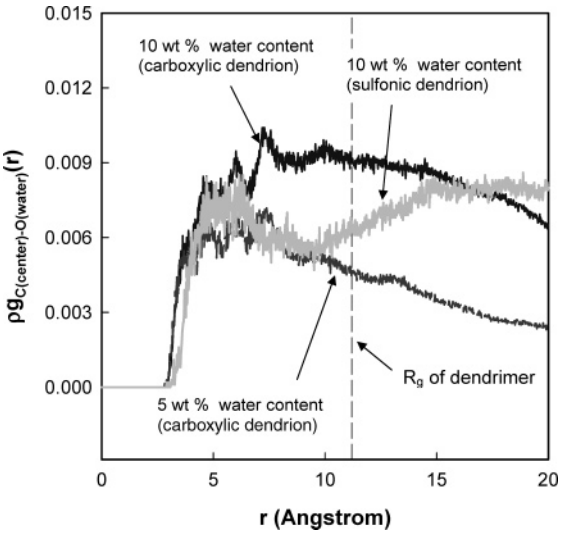

Figure 10. Product of pair correlation functions of the central carbon of dendrimer and oxygen in water, $g_{C(center)-O(water)}(r)$ with water number density (ρ). The numbers of waters inside the dendrimer are 51.2 and 31.3 for the 10 and 5 wt % water content, respectively, in the carboxylic dendrion membrane and 34.7 for the 10 wt % water content in the sulfonic dendrion membrane.

for the 10 wt % water content. The first distinct difference between the carboxylic dendrion and the sulfonic dendrion is the thickness of the first solvation shell: As shown in Figure 9, for carboxylic acid, the thickness of the first water shell is 3 Å from $g_{C(acid)-O(water)}(r)$, whereas the thickness of the shell for sulfonic acid is 1.5 Å, which is comparable to 2 Å for the case of Nafion in our previous study.[28] We think that this difference is attributed to the complete ionization of the sulfonic acid that produces a more compact solvation layer. From the water coordination number and the volume of such solvation shell, the density of water in the first solvation shell was calculated as 0.28 g/cm^3 for the 10 wt % case and 0.12 g/cm^3 for the 5 wt % water content in the carboxylic dendrion membrane and 0.49 g/cm^3 for the 10 wt % water content in the sulfonic dendrion membrane.

Above, we discussed water that solvates the hydrophilic moieties of the dendrimer. But, what about the water inside dendrimer? From the dendritic architecture, we expect some free volume available inside the dendrimer for a water phase. Figure 10 shows a plot of water density around the central carbon of the dendrimer ($C_{(center)}$ shown in Figure 1), $\rho g_{C(center)-O(water)}(r)$. The vertical dashed line denotes the radius of gyration of the dendrimer. We see that, for the carboxylic dendrion membrane, the 10 wt % water dendrion has 51.2 water inside dendrimer (within the radius of gyration), while the 5 wt % case has 31.3. For the sulfonic dendrion membrane, it has 34.7. Although the benzyl ether moieties are not particularly hydrophilic, they are certainly less hydrophobic than the perfluorocarbon chain (PTFE). Thus, water in the internal space of the dendrimer will prefer benzyl ether, which is less hydrophobic than PTFE. In this context, these structures resemble reversed micelles in which the water phase is contained in the dendrimer blocks surrounded by the hydrophobic PTFE matrix, similar to the morphological characteristics of the Nafion membrane.

3.4. Structure Factors. To quantify the extent of phase segregation, we calculate the structure factor, $S(q)$ as obtained in small-angle scattering experiments (SAXS and SANS), using the following equation

$$\mathbf{S}(\mathbf{q}) = \langle \sum_{r_i} \sum_{r_j} \exp(i\mathbf{q}\cdot\mathbf{r}_{ij})(\xi^i\xi^j - \langle\xi\rangle^2)\rangle/L^3 \qquad (3)$$

where the angular bracket denotes a thermal statistical average, ξ^i represents a local density contrast, $(\phi_A{}^j - \phi_B{}^j)$, and $\mathbf{q}$ and $\mathbf{r}_{ij}$ are the scattering vector and the vector between sites i and j, respectively. This analysis has been used successfully in other simulations to investigate the phase-segregated structure in copolymer systems[79−82] and polymer blend systems.[83−88] Analysis of SAXS experiments uses the electron density contrast and SANS experiments uses deuterium density contrast. For our analysis, we assigned an artificial density contrast as follows. The local density variable $\phi_A{}^j$ is equal to 1 if the site j is occupied by a hydrophilic entity such as water and equal to 0 otherwise, and $\phi_B{}^j$ is equal to 1 if the site is occupied by hydrophobic entities such as PTFE backbone and equal to 0 otherwise. The quantity $\mathbf{S}(\mathbf{q})$ is spherically averaged as follows:

$$S(q) = \sum_{|\mathbf{q}|} \mathbf{S}(\mathbf{q}) / \sum_{|\mathbf{q}|} 1 \qquad (4)$$

with $q = (2\pi/L)n$, where $n = 1, 2, 3, \cdots$ denotes that, for a given n, a spherical shell is taken as $n - {}^1/_2 \le qL/2\pi \le n + {}^1/_2$.

In our previous study using this analysis on the hydrated Nafion membrane,[28] we computed a characteristic dimension of nanophase segregation of ∼30−50 Å, which is quite comparable with the experimental observations (∼50 Å). For the dendrion, this method leads to the structure factor profiles as a function of scattering vector, $\mathbf{q}$, shown in Figure 11. These structure profiles are calculated for the *large* system consisting of 32 copolymer molecules as mentioned in section 2. This is because the small system consisting of 4 copolymers would not allow the structural development of the phase segregation beyond its system size (∼40 Å corresponding to $q = \sim 0.15$ Å^{-1}).

The structure factor analysis in Figure 11 leads to a maximum intensity at ∼0.2 Å^{-1} for both water contents, indicating that the characteristic dimension of phase segregation in the new copolymer membrane is around 30 Å. Because we found that water molecules are incorporated with the hydrophilic dendrimer of the same size for both water contents in the membrane, we conclude that the characteristic dimension of the water phase is insensitive to the water content up to 10 wt %. Thus, the main difference in the structure factor profile for the two water contents is the intensity of the structure factor up to 0.3 Å^{-1} reflecting the concentration contrast. Indeed, in Figure 11, the maximum of $S(q)$ of the 10 wt % water content is nearly two times larger than that of the 5 wt % water content. This result is consistent with all other results presented in Figures 10 and 12. From this result, we confirm again that the nanophase segregation of the dendrion copolymer is dominated by the connected dendritic architecture.

4. Water Dynamics

Most critical to the performance of PEMFC is the proton conductivity (which we want to be large) and the water diffusion. The former is especially dependent on the rotational dynamics of water molecules to facilitate a continuously evolving proton hopping. Although the role of water rotation in the hydrated membrane is essential for a fundamental understanding of proton conduction, it has been analyzed very little. Probably, this is due to the lack of experimental tools to directly measure this phenomenon in the membrane. Here, we

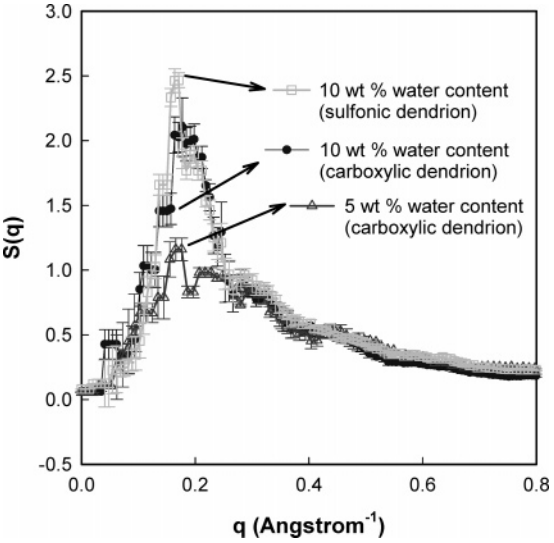

Figure 11. Structure factor profile for hydrated copolymer membrane with 10 and 5 wt % water content simulated at 353.15 K. This shows that the characteristic dimension of nanophase-segregated structure is ~30 Å ($q = 0.2$ Å^{-1}) for both water contents (10 and 5 wt %).

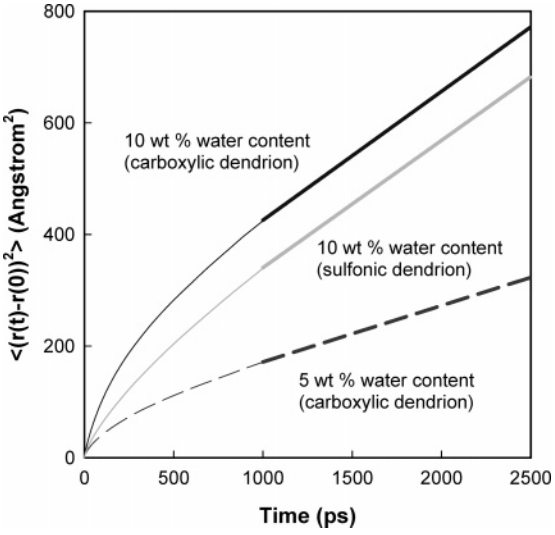

Figure 12. Mean-squared displacement as a function of time of water in the hydrated copolymer system simulated at 353.15 K for 5 ns.

will analyze the rotational water dynamics in the hydrated dendrion membrane and compare it with the values computed and measured for bulk water.

A second important feature of water dynamics in the hydrated membrane is the translational diffusion coefficient. If the membrane leads a high electroosmotic drag coefficient, it may be necessary to have a high value of translational diffusion for water to regulate a uniform water distribution by concentration-gradient-driven drift toward the anode. Inversely, we expect that the electroosmotic drag of water by the protons would be difficult in an environment having low translational mobility of water. An example is the ice near the melting point where the translational diffusion of water is strongly restricted while the rotational degree of freedom is active.

Previously,[28] we showed that the membrane transport properties depend on the extent of nanophase segregation between hydrophilic and hydrophobic phases, in agreement with experimental observations.[2,67,89] For PEMFC applications, we want to minimize water mobility in order to reduce the electroosmotic drag of water as protons are transported from anode to cathode. Otherwise, the membrane near the anode can become too dry, while the membrane near the cathode floods, producing uneven and unpredictable changes in the conductivity of the membrane during operation of the cell. Thus, we prefer that water in the membrane has a bulklike water phase that percolates throughout the membrane to aid proton transport while simultaneously minimizing translational transport.

TABLE 2: Rotational Diffusion Coefficients (D_R's) of Water from the MD Simulations[a]

system		D_R ($\times 10^{11}$/s) $T =$ 298.15 K	D_R ($\times 10^{11}$/s) $T =$ 353.15 K
bulk water		3.25 ± 0.24 (exp. 2.2[b])	7.05 ± 0.42
carboxylic dendrion	5 wt % water content		12.24 ± 0.53
	10 wt % water content		7.34 ± 0.51
sulfonic dendrion	10 wt % water content		7.49 ± 0.45
Nafion	20 wt % water content DR = 1.1		7.42 ± 0.54
	20 wt % water content DR = 0.1		6.23 ± 0.53

[a] This is expected to correlate with proton transport rates. [b] Reference 91.

This next section analyzes water dynamics from the 5-ns NPT MD simulation in terms of the rotational and translational diffusion.

4.1. Calculations of Rotational Diffusion. To determine the rotational dynamics of water, we calculated the rotational diffusion coefficient (D_R) as[90]

$$D_R = \frac{kTS(0)}{12N} \tag{5}$$

where k is the Boltzmann constant, T is absolute temperature, and N is the number of water molecules. $S(0)$ in eq 5 is the rotational density of states at zero frequency

$$S(v)]_{v=0} = \frac{2}{kT} \lim_{\tau-\infty} \int_{-\tau}^{\tau} C_R(t)\, e^{-i2\pi vt}\, dt]_{v=0} \tag{6}$$

Here, $C_R(t)$ is the autocorrelation function of angular velocity, $\omega_{ij}^{CM}(t)$ of water molecule (i)

$$C_R(t) = \sum_{j=1}^{3} c_{R_j}(t) = \sum_{i=1}^{n}\sum_{j=1}^{3} \langle \omega_{ij}^{CM}(t)\, \omega_{ij}^{CM}(0)\rangle \tag{7}$$

This analysis allows us to evaluate how the rotational diffusion of water molecules is affected by the dendrion.

As summarized in Table 2, we calculate a rotational diffusion rate (D_R) for pure bulk water of $(3.25 \pm 0.24) \times 10^{11}$/s, which is comparable to the experimental value[91] of 2.2×10^{11}/s at the same temperature of 298.15 K. For the higher temperature of 353.15 K, we predict that D_R of bulk increases by a factor of 2.2 (to $(7.05 \pm 0.42) \times 10^{11}$/s) (we have not found an experimental value at this higher temperature).

For the carboxylic dendrion at 353.15 K, we calculate that the D_R of water is $(7.34 \pm 0.51) \times 10^{11}$/s for 10 wt % water content and $(12.24 \pm 0.53) \times 10^{11}$/s for 5 wt % water content, and for the sulfonic dendrion, it is $(7.49 \pm 0.45) \times 10^{11}$/s for 10 wt % water content. Thus, for 10 wt % water content, we predict that the D_R of water in the dendrion is within 5% of the value calculated for bulk water. The ~70% increase in the rotational diffusion coefficient of water as the water content is decreased from 10% to 5% suggests that the average hydrogen bond to the water molecules weakens with decreasing water content,[3,65,67] which is consistent with the water structure analyses in section 3.2.

TABLE 3: Translational Diffusion Coefficients of Water from MD Simulations

system		D_T ($\times 10^5$ cm^2/s) $T =$ 298.15 K	$T =$ 353.15 K
bulk water		2.69 ± 0.04 (exp. 2.30[a])	5.98 ± 0.07 (exp. 6.48[a])
carboxylic dendrion	5 wt % water content		0.26 ± 0.04
	10 wt % water content		0.54 ± 0.07
sulfonic dendrion	10 wt % water content		0.37 ± 0.06
Nafion	20 wt % water content DR = 1.1		1.43 ± 0.07[b] (1.25[c])
	20 wt % water content DR = 0.1		1.62 ± 0.05[b] (1.25[c])

[a] References 92−94. [b] Reference 28. [c] Reference 101.

We also find that with 10 wt % water content the water rotation in the dendrion is comparable with the value for 20 wt % hydrated Nafion. This is consistent with the results from the structural investigation on the dendrion, which indicate that 10% hydrated dendrion has a water structure comparable to 20% hydrated Nafion membrane. Although we consider rotational diffusion essential for continuous evolution of proton hopping, it is not the only factor governing the proton transfer. Another major factor for proton hopping is the distance between proton-donating oxygen and proton-accepting oxygen, R(D−A), which will be discussed in section 5. This factor is optimized in the compact hydrogen-bonding network of bulk water. These two factors, rotational diffusion and R(D−A), are competitive, because the rotational diffusion of water is slowed by a strong compact hydrogen bond network. However, for systems with similar water structure (such as Nafion with 20 wt % water and dendrion with 10 wt % water), we expect that the relative proton transfer rates will be dominated by rotational diffusion.

4.2. Calculations of Translational Diffusion. To analyze the effect of the dendrion architecture on water transport properties, we calculated the mean-square displacement (MSD) of water from the 5-ns trajectories as shown in Figure 12. Using $\langle[r(t) - r(0)]^2\rangle = 6D_T t$ with the linear part of MSD in Figure 12, we calculate the translational diffusion coefficients (D_T's) for water as summarized in Table 3. The calculated values of D_T in bulk water are $(2.69 \pm 0.04) \times 10^{-5}$ cm^2/s at 298.15 K and $(5.98 \pm 0.07) \times 10^{-5}$ cm^2/s at 353.15 K, which agree reasonably well with the experimental values (2.30×10^{-5} cm^2/s at 298.15 K and 6.48×10^{-5} cm^2/s at 353.15 K).[92−94]

The diffusion coefficient (D_T) of water at 353.15 K is as follows: For the carboxylic dendrion, $D_T = (0.54 \pm 0.07) \times 10^{-5}$ cm^2/s for 10 wt % water content and $(0.26 \pm 0.04) \times 10^{-5}$ cm^2/s for 5 wt % water content. For the sulfonic dendrion, $D_T = (0.37 \pm 0.06) \times 10^{-5}$ cm^2/s for 10 wt % water content. Although D_T increases by a factor of 2 as the water content increases from 5% to 10%, the latter value remains a factor of 11 smaller than the calculated value for bulk water. These results are comparable with those[28] for hydrated Nafion with water content of 20 wt %. These results can be compared with those[28] for hydrated Nafion with water content of 20 wt %: $D_T = (1.43 \pm 0.07) \times 10^{-5}$ cm^2/s for the monomeric sequence DR = 1.1 and $(1.62 \pm 0.05) \times 10^{-5}$ cm^2/s for DR = 0.1. Thus, with 10% water content in the dendrion, D_T of water is only ∼25−36% of that for 20% hydrated Nafion. We expect, therefore, that the electroosmotic drag in an ionized dendrion may be substantially smaller than in the Nafion-based membrane

In summary, the structure of the water phase in the dendrion reaches a bulklike state at $^1/_2$ the water content as the hydrated Nafion membrane, but the dendrion has $\sim^1/_4-^1/_3$ the translational diffusion coefficient.

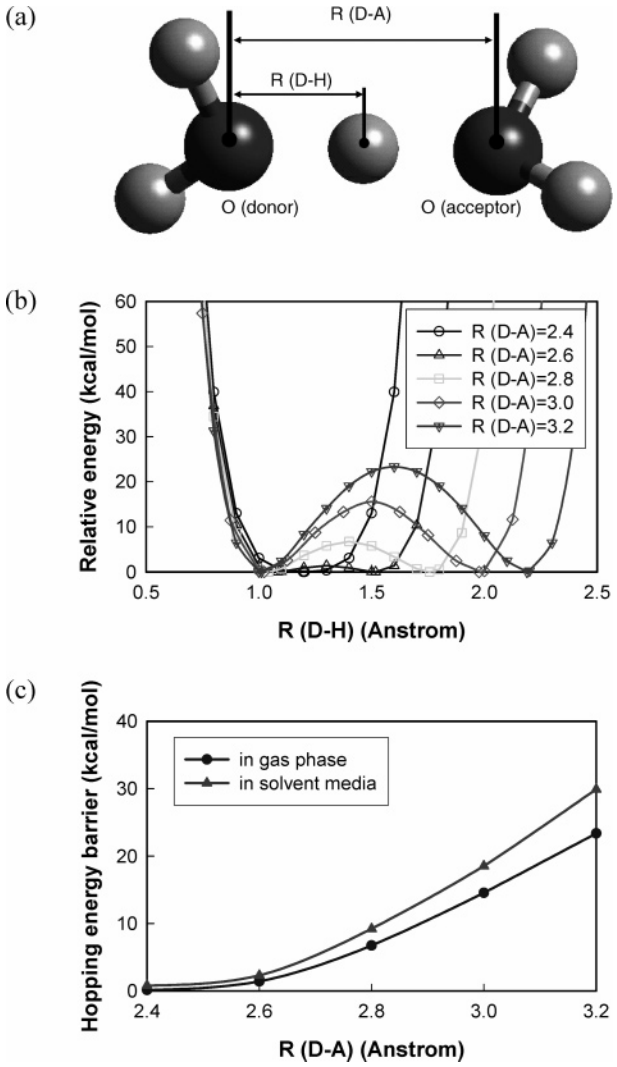

Figure 13. (a) Proton hopping from a water to another, (b) relative energy change as a function of distance between oxygen in donor and proton, and (c) change of hopping energy barrier with increasing distance between oxygen in donor and oxygen in acceptor.

5. Proton Transport

In the water channel of these membranes, protons are transported through two different mechanisms: the diffusion of protonated water molecules (vehicular diffusion) and the hopping of the proton along sequences of water molecules (Grothuss diffusion). In contrast to the former, which can be handled in a classical MD scheme using $D_{vehicular} = \langle[r(t) - r(0)]^2\rangle/6t$, the latter requires us to consider a quantum description of proton movement from a hydronium molecule to a neighboring water. Although accurate MD methodology such as ab initio MD has been used to investigate the transport of protons in water,[68,69] we employ a simple and efficient method based on transition state theory (TST) to estimate the contribution from the proton hopping mechanism to proton diffusion, which has been successfully used in our group to investigate proton hopping between imidazole molecules.[95]

To calculate the hopping diffusion in the membrane, we first parametrized the rate constant for the transfer of a proton from the protonated water (hydronium) to the neutral carrier as a function of the intermolecular oxygen in the donor and the

TABLE 4: Proton Diffusion Coefficients (*D*'s)

system ($T = 353.15$ K)			$D_{vehicular}$ (10^{-5} cm^2/s)	$D_{hopping}$ (10^{-5} cm^2/s)	D_{total} (10^{-5} cm^2/s)
sulfonic dendrion		10 wt % water content	0.141	0.377	0.518
	DR = 1.1	20 wt % water content	0.290[a]	0.342	0.632 (exp. ~0.5−0.7)[b]
	DR = 0.1	20 wt % water content	0.294[a]	0.407	0.701 (exp. ~0.5−0.7)[b]

[a] Reference 28. [b] References 66 and 100.

oxygen in the acceptor distance (Figure 13a) using the following equation[96,97]

$$k_{ij}(r) = \kappa(T, r)\frac{k_B T}{h}\exp\left(-\frac{E_{ij}(r) - 1/2h\omega(r)}{RT}\right) \qquad (8)$$

where $\kappa(T, r)$ and $\omega(r)$ are the tunneling factor and the frequency for zero-point energy correction (given in refs 96 and 97) and $E(r)$ is the energy barrier for the proton to be transferred from donor to acceptor in the water medium while they are at a distance r. To assess this hopping energy barrier, first, we obtained the relative energy change as a function of the distance between the oxygen (donor) and the proton, at a given distance between the oxygen in the donor and the oxygen in the acceptor using the B3LYP/6-311G** level (Figure 13b), and then, we calculated the energy barrier with the solvent effect correction using the Poisson−Boltzmann self-consistent reaction field model (Figure 13c).[98,99] The hopping diffusion coefficient was calculated as follows:

$$D_{hopping} = \frac{1}{6Nt}\int_0^{t\to\infty}\sum_i^N\sum_j^M k_{ij} r_{ij}^2 P_{ij}\, dt \qquad (9)$$

where N is the number of protons and P_{ij} is the probability with which a proton can jump from hydronium i to water j defined as $P_{ij} = k_{ij}/\Sigma_j^M k_{ij}$. Here, r_{ij} is the distance between all the pairs of donors and acceptors measured from the equilibrium molecular dynamics trajectory. As summarized in Table 4, we found that $D_{hopping}$ for the sulfonic dendrion membrane with 10 wt % water content is comparable to the Nafion membrane with 20 wt % water content. Table 4 also shows the estimated total proton diffusion coefficient ($D_{total} = D_{vehicular} + D_{hopping}$) for this new membrane in comparison with the given Nafion membrane. We see that the values of D_{total} calculated from the hydrated Nafion membrane in our previous study[28] (0.632×10^{-5} cm^2/s for DR = 1.1 and 0.701×10^{-5} cm^2/s for DR = 0.1) are in very good agreement with the experimental observations reported from Zawodzinski et al. ($\sim 0.5 \times 10^{-5}$ cm^2/s)[100] and from Kreuer ($\sim 0.7 \times 10^{-5}$ cm^2/s),[66] which indicates that our simulations describe well the proton transport in the hydrated membrane system. In addition, comparing D_{total} between the sulfonic dendrion membrane and the Nafion membrane, we find that the sulfonic dendrion membrane with 10 wt % water content has almost the same level of proton diffusion as the Nafion membranes. Because the Nafion membrane with high water content (>20 wt %) has 0.1 S/cm of specific conductivity, we expect this sulfonic dendrion membrane to have ~0.08 S/cm at one-half the level in water content.

6. Conclusions

We introduce the dendrion concept of using precisely defined water-soluble dendritic architecture in a copolymer with a hydrophobic polymer backbone to achieve nanophase segregation and transport suitable for applications such as PEMFC. In particular, we consider here the dendrion in which the second-generation Fréchet dendrimer is covalently connected with a hydrophobic linear PTFE. We studied the structures and properties of this system using full atomistic MD simulations, leading to results that suggest that this dendrion class of copolymers presents a robust nanophase segregation controlled by the architecture of the molecule that makes them promising materials for fuel cell membranes.

We considered hydration of the dendrion with 10 and 5 wt % water content, where we find a well-developed nanophase-segregated structure consisting of a hydrophobic PTFE phase and a hydrophilic Fréchet dendrimer phase including the water. The size of the dendrimer was ~11 Å (radius of gyration), independent of the water content. This analysis also suggests that the dendrimers contact each other in the hydrated membrane, helping to establish a continuous water nanophase. These structures resemble reversed micelles, where the water phase is contained in the dendrimer blocks. It should be emphasized, however, that the water nanophase in the dendrion also covers and connects the hydrophilic dendrimers, rendering a continuous water nanophase, essential for the prospect of proton transport in an ionizable dendrion copolymer.

For the 10 wt % water content case, we found that the water coordination numbers are 7.3 for the carboxylic acid and 4.4 for the sulfonic acid, while for 5 wt % water, it is 3.1 for carboxylic acid. From this analysis, we conclude that, at 10 wt % water content, the additional waters incorporate mainly with the polar group in the dendrimer periphery and the internal space of the dendrimer without increasing the size of the water phase in the nanophase-segregated membrane.

We found that, within R_g of each dendrimer, there are ~51 water molecules for the carboxylic dendrion and ~35 for the sulfonic dendrion, while for the 5 wt % case in carboxylic dendrion, there are ~31. This shows that the water molecules can stay inside the dendrimer.

The extent of nanophase segregation in the new copolymer membrane was evaluated quantitatively by analyzing structure factor profiles, $\mathbf{S}(\mathbf{q})$ as a function of scattering vector ($\mathbf{q}$). For both water contents, we find a maximum in $\mathbf{S}(\mathbf{q})$ at $\mathbf{q} = \sim 0.2$ Å^{-1}, corresponding to a characteristic dimension for phase segregation of ~30 Å. But in the 10 wt % case, the intensity at this $\mathbf{q}$ is twice that for the 5 wt % case. This indicates that the characteristic dimension of phase segregation in the hydrated membrane is not sensitive to the change in water content, while the concentration contrast depends on the water content. This result is reasonable, because the water molecules distribute to solvate the hydrophilic part of the dendrimer whose distribution in the system is almost independent of water content. This result is consistent with other analyses in this study. In conclusion, the nanophase segregation is dominated by the dendritic architecture, and the capacity of the dendrimer to accommodate water inside its structure contributes to the robustness of the dimensions of phase segregation observed in these systems.

To determine the structure of the water phase, we analyzed the pair correlation function of the water oxygen pairs. We find that the water structure approaches that of bulk water at half

the water loading (10 wt %) required for hydrated Nafion membrane (20 wt %).

Calculating D_R from its angular velocity autocorrelation function, we find that the D_R of water in the dendrion has a larger value at a lower water content. This occurs because the hydrogen bond network becomes looser with decreasing water content (in agreement with the water coordinate number in the water phase in Figure 7). In the dendrion, the value of D_R for water converges to that of bulk water at the 10 wt % water content.

We calculated the translational diffusion coefficient (D_T) of water in the dendrion to be $\sim^1/_4-^1/_3$ of the value for hydrated Nafion membrane with similar water contents. This suggests that the dendrion should lead to lower electroosmotic drag and improved water management compared to Nafion.

We estimated the proton diffusion according to its mechanism: vehicular and hopping. Particularly, the hopping diffusion coefficient ($D_{hopping}$) for the sulfonic dendrion with 10 wt % water content is very comparable to that for the Nafion with 20 wt % water, and thereby, the total proton diffusion (D_{total}) is also so.

Our conclusion is that the dendrion diblock copolymer consisting of a Fréchet dendrimer combined with linear PTFE can have membrane properties for structure and transport that are comparable to those of hydrated Nafion but at half the water content, which makes it a promising candidate as a high-performance membrane for fuel cell applications.

Acknowledgment. We thank Dr. Gerald Voecks of General Motors for many helpful discussions. The facilities of the Materials and Process Simulation Center used for these studies are supported by DURIP-ARO, DURIP-ONR, IBM-SUR, and NSF (MRI), and other support for the MSC comes from MURI-ARO, MURI-ONR, DOE, ONR, NSF-CSEM, NIH, General Motors, Chevron-Texaco, Seiko-Epson, Beckman Institute, and Asahi Kasei.

References and Notes

(1) Carrette, L.; Friedrich, K. A.; Stimming, U. *ChemPhysChem* **2000**, *1*, 162−193.
(2) Kreuer, K. D. *J. Membr. Sci.* **2001**, *185*, 29−39.
(3) Paddison, S. J. *Annu. Rev. Mater. Res.* **2003**, *33*, 289−319.
(4) Li, Q.; He, R.; Jensen, J. O.; Bjerrum, N. J. *Chem. Mater.* **2003**, *15*, 4896−4915.
(5) Eisenberg, A., Yeager, H. L., Eds. *Perfluorinated Ionomer Membranes*; American Chemical Society: Washington, DC, 1982.
(6) Yeager, H. L.; Steck, A. *Anal. Chem.* **1979**, *51*, 862−865.
(7) Yeo, S. C.; Eisenberg, A. *J. Appl. Polym. Sci.* **1977**, *21*, 875−898.
(8) Eisenberg, A.; King, M. In *Polymer Physics*; Stein, R. S., Ed.; Academic Press: New York, 1977.
(9) Scibona, G.; Fabiani, C.; Scuppa, B. *J. Membr. Sci.* **1983**, *16*, 37−50.
(10) Eisenberg, A. *Macromolecules* **1970**, *3*, 147−154.
(11) Falk, M. *Can. J. Chem.* **1980**, *58*, 1495−1501.
(12) Duplessix, R.; Escoubes, M.; Rodmacq, B.; Volino, F.; Roche, E.; Eisenberg, A.; Peneri, M. In *Water in Polymer*; American Chemical Soceity: Washington, DC, 1980.
(13) Rodmacq, B.; Coey, J. M.; Escoubes, M.; Roche, E.; Duplessix, R.; Eisenberg, A.; Pineri, M. In *Water in Polymers*; Rowland, S. P., Ed.; American Chemical Society: Washington, DC, 1980.
(14) Gierke, T. D.; Munn, G. E.; Wilson, F. C. *J. Polym. Sci., Polym. Phys. Ed.* **1981**, *19*, 1687−1704.
(15) Hsu, W. Y.; Gierke, T. D. *J. Membr. Sci.* **1983**, *13*, 307−326.
(16) Yeager, H. L.; Steck, A. *J. Electrochem. Soc.* **1981**, *128*, 1880−1884.
(17) Verbrugge, M. W.; Hill, R. F. *J. Electrochem. Soc.* **1990**, *137*, 886−893.
(18) Gebel, G. *Polymer* **2000**, *41*, 5829−5838.
(19) James, P. J.; Elliott, J. A.; McMaster, T. J.; Miles, J. M. *J. Mater. Sci.* **2000**, *35*, 5111−5119.
(20) James, P. J.; McMaster, T. J.; Newton, J. M.; Miles, M. J. *Polymer* **2000**, *41*, 4223−4231.
(21) Haubold, H.-G.; Vad, T.; Jungbluth, H.; Hiller, P. *Electrochim. Acta* **2001**, *46*, 1559−1563.
(22) Rollet, A.-L.; Gebel, G.; Simonin, J.-P.; Turq, P. *J. Polym. Sci., Part B: Polym. Phys.* **2001**, *39*, 548−558.
(23) Rollet, A.-L.; Diat, O.; Gebel, G. *J. Phys. Chem. B* **2002**, *106*, 3033−3036.
(24) Young, S. K.; Trevino, S. F.; Tan, N. C. B. *J. Polym. Sci., Part B: Polym. Phys.* **2002**, *40*, 387−400.
(25) Tovbin, Y. K.; Dyakov, Y. A.; Vasutkin, N. F. *Russ. J. Phys. Chem. (Engl. Transl.)* **1993**, *67*, 2122−2125.
(26) Dyakov, Y. A.; Tovbin, Y. K. *Russ. Chem. Bull.* **1995**, *44*, 1233−1236.
(27) Vishnyakov, A.; Neimark, A. V. *J. Phys. Chem. B* **2001**, *105*, 7830−7834.
(28) Jang, S. S.; Molinero, V.; Cagin, T.; Goddard, W. A., III *J. Phys. Chem. B* **2004**, *108*, 3149−3157.
(29) Grayson, S. M.; Frechet, J. M. J. *Chem. Rev.* **2001**, *101*, 3819−3867.
(30) Frechet, J. M. J. *J. Polym. Sci., Part A: Polym. Chem.* **2003**, *41*, 3713−3725.
(31) Frechet, J. M. J. *Macromol. Symp.* **2003**, *201*, 11−22.
(32) Hawker, C. J.; Wooley, K. L.; Frechet, J. M. J. *J. Chem. Soc., Perkin Trans. 1* **1993**, 1287−1297.
(33) Gitsov, I.; Frechet, J. M. J. *Macromolecules* **1993**, *26*, 6536−6546.
(34) Gitsov, I.; Wooley, K. L.; Hawker, C. J.; Ivanova, P. T.; Frechet, J. M. J. *Macromolecules* **1993**, *26*, 5621−5627.
(35) Debrabandervandenberg, E. M. M.; Meijer, E. W. *Angew. Chem., Int. Ed. Engl.* **1993**, *32*, 1308−1311.
(36) Frechet, J. M. J.; Hawker, C. J.; Wooley, K. L. *J. Macromol. Sci., Pure Appl. Chem.* **1994**, *A31*, 1627−1645.
(37) Chapman, T. M.; Hillyer, G. L.; Mahan, E. J.; Shaffer, K. A. *J. Am. Chem. Soc.* **1994**, *116*, 11195−11196.
(38) Frechet, J. M. J.; Gitsov, I. *Macromol. Symp.* **1995**, *98*, 441−465.
(39) Vanhest, J. C. M.; Baars, M.; Elissenroman, C.; Vangenderen, M. H. P.; Meijer, E. W. *Macromolecules* **1995**, *28*, 6689−6691.
(40) Aoi, K.; Motoda, A.; Okada, M.; Imae, T. *Macromol. Rapid Commun.* **1997**, *18*, 945−952.
(41) Iyer, J.; Fleming, K.; Hammond, P. T. *Macromolecules* **1998**, *31*, 8757−8765.
(42) Iyer, J.; Hammond, P. T. *Langmuir* **1999**, *15*, 1299−1306.
(43) Johnson, M. A.; Santini, C. M. B.; Iyer, J.; Satija, S.; Ivkov, R.; Hammond, P. T. *Macromolecules* **2002**, *35*, 231−238.
(44) Istratov, V.; Kautz, H.; Kim, Y. K.; Schubert, R.; Frey, H. *Tetrahedron* **2003**, *59*, 4017−4024.
(45) Roman, C.; Fischer, H. R.; Meijer, E. W. *Macromolecules* **1999**, *32*, 5525−5531.
(46) Mayo, S. L.; Olafson, B. D.; Goddard, W. A. *J. Phys. Chem.* **1990**, *94*, 8897−8909.
(47) Elliott, J. A.; Hanna, S.; Elliott, A. M. S.; Cooley, G. E. *Phys. Chem. Chem. Phys.* **1999**, *1*, 4855.
(48) Vishnyakov, A.; Neimark, A. V. *J. Phys. Chem. B* **2000**, *104*, 4471−4478.
(49) Li, T.; Wlaschin, A.; Balbuena, P. B. *Ind. Eng. Chem. Res.* **2001**, *40*, 4789−4800.
(50) Jang, S. S.; Blanco, M.; Goddard, W. A., III; Caldwell, G.; Ross, R. B. *Macromolecules* **2003**, *36*, 5331−5341.
(51) Levitt, M.; Hirshberg, M.; Sharon, R.; Laidig, K. E.; Daggett, V. *J. Phys. Chem. B* **1997**, *101*, 5051−5061.
(52) Rappe, A. K.; Goddard, W. A., III *J. Phys. Chem.* **1991**, *95*, 3358−3363.
(53) Hockney, R. W.; Eastwood, J. W. *Computer simulation using particles*; McGraw-Hill International Book Co.: New York, 1981.
(54) Plimpton, S. J. *J. Comput. Phys.* **1995**, *117*, 1−19.
(55) Plimpton, S. J.; Pollock, R.; Stevens, M. In *The Eighth SIAM Conference on Parallel Processing for Scientific Computing*; Minneapolis, MN, 1997.
(56) Jang, S. S.; Lin, S.-T.; Maiti, P. K.; Blanco, M.; Goddard, W. A., III; Shuler, P.; Tang, Y. *J. Phys. Chem. B* **2004**, *108*, 12130−12140.
(57) Verlet, L. *Phys. Rev.* **1967**, *159*, 98−103.
(58) *Cerius*^{2}, version 4.0; Accelrys, Inc.: San Diego, CA, 1999.
(59) Nose, S. *J. Chem. Phys.* **1984**, *81*, 511.
(60) Topp, A.; Bauer, B. J.; Tomalia, D. A.; Amis, E. J. *Macromolecules* **1999**, *32*, 7232−7237.
(61) Evmenenko, G.; Bauer, B. J.; Keppinger, R.; Forier, B.; Dehaen, W.; Amis, E. J.; Mischenko, N.; Reynaers, H. *Macromol. Chem. Phys.* **2001**, *202*, 891−899.
(62) Maiti, P. K.; Cagin, T.; Wang, G. F.; Goddard, W. A., III *Macromolecules* **2004**, *37*, 6236−6254.
(63) Agmon, N. *Chem. Phys. Lett.* **1995**, *244*, 456−462.
(64) Agmon, N.; Goldberg, S. Y.; Huppert, D. *J. Mol. Liq.* **1995**, *64*, 161−195.
(65) Kreuer, K.-D. *Chem. Mater.* **1996**, *8*, 610−641.
(66) Kreuer, K. D. *Solid State Ionics* **1997**, *97*, 1−15.

(67) Kreuer, K. D. *Solid State Ionics* **2000**, *136*−*137*, 149−160.
(68) Tuckerman, M.; Laasonen, K.; Sprik, M.; Parrinello, M. *J. Chem. Phys.* **1995**, *103*, 150−161.
(69) Tuckerman, M.; Laasonen, K.; Sprik, M.; Parrinello, M. *J. Phys. Chem.* **1995**, *99*, 5749−5752.
(70) Tuckerman, M. E.; Marx, D.; Klein, M. L.; Parrinello, M. *Science* **1997**, *275*, 817−820.
(71) Marx, D.; Tuckerman, M. E.; Hutter, J.; Parrinello, M. *Nature (London)* **1999**, *397*, 601−604.
(72) Marx, D.; Tuckerman, M. E.; Parrinello, M. *J. Phys.: Condens. Matter* **2000**, *12*, A153−A159.
(73) Verbrugge, M. W.; Hill, R. F. *J. Electrochem. Soc.* **1990**, *137*, 893−899.
(74) Verbrugge, M. W.; Hill, R. F. *J. Electrochem. Soc.* **1990**, *137*, 3770−3777.
(75) Zawodzinski, T. A.; Neeman, M.; Sillerud, L. O.; Gottesfeld, S. *J. Phys. Chem.* **1991**, *95*, 6040−6044.
(76) Soper, A. K.; Phillips, M. G. *Chem. Phys.* **1986**, *107*, 47−60.
(77) Marti, J.; Padro, J. A.; Guardia, E. *J. Chem. Phys.* **1996**, *105*, 639−649.
(78) Wernet, P.; Nordlund, D.; Bergmann, U.; Cavalleri, M.; Odelius, M.; Ogasawara, H.; Naslund, L. A.; Hirsch, T. K.; Ojamae, L.; Glatzel, P.; Pettersson, L. G. M.; Nilsson, A. *Science* **2004**, *304*, 995−999.
(79) Fried, H.; Binder, K. *J. Chem. Phys.* **1991**, *94*, 8349−8366.
(80) Molina, L. A.; Rodriguez, A. L.; Freire, J. J. *Macromolecules* **1994**, *27*, 1160−1165.
(81) Hoffmann, A.; Sommer, J.-U.; Blumen, A. *J. Chem. Phys.* **1997**, *106*, 6709−6721.
(82) Jo, W. H.; Jang, S. S. *J. Chem. Phys.* **1999**, *111*, 1712−1720.
(83) Binder, K. *Colloid Polym. Sci.* **1987**, *265*, 273−288.
(84) Sariban, A.; Binder, K. *J. Chem. Phys.* **1987**, *86*, 5859−5873.
(85) Chakrabarti, A.; Toral, R.; Gunton, J. D.; Muthukumar, M. *J. Chem. Phys.* **1990**, *92*, 6899−6909.
(86) Sariban, A.; Binder, K. *Macromolecules* **1991**, *24*, 578−592.
(87) Brown, G.; Chakrabarti, A. *Phys. Rev. E* **1993**, *48*, 3705−3711.
(88) Jo, W. H.; Kim, J. G.; Jang, S. S.; Youk, J. H.; Lee, S. C. *Macromolecules* **1999**, *32*, 1679−1685.
(89) Schuster, M.; Kreuer, K. D.; Maier, J. In *14th international conference on solid state ionics*: Monterey, USA, 2003; p 395.
(90) McQuarrie, A. A. *Statistical Mechanics*; Harper & Row: New York, 1976.
(91) Pal, S. K.; Peon, J.; Bagchi, B.; Zewail, A. H. *J. Phys. Chem. B* **2002**, *106*, 12376−12395.
(92) Mills, R. *J. Phys. Chem.* **1973**, *77*, 685−688.
(93) Krynicki, K.; Green, C. D.; Sawyer, D. W. *Discuss. Faraday Soc.* **1978**, *66*, 199−208.
(94) Price, W. S.; Ide, H.; Arata, Y. *J. Phys. Chem. A* **1999**, *103*, 448−450.
(95) Deng, W.-Q.; Molinero, V.; Goddard, W. A., III *J. Am. Chem. Soc.* **2004**, *126*, 15644−15645.
(96) Lill, M. A.; Helms, V. *J. Chem. Phys.* **2001**, *114*, 1125−1132.
(97) Lill, M. A.; Helms, V. *J. Chem. Phys.* **2001**, *115*, 7985−7992.
(98) Greeley, B. H.; Russo, T. V.; Mainz, D. T.; Friesner, R. A.; Langlois, J. M.; Goddard, W. A.; Donnelly, R. E.; Ringnalda, M. N. *J. Chem. Phys.* **1994**, *101*, 4028−4041.
(99) Marten, B.; Kim, K.; Cortis, C.; Friesner, R. A.; Murphy, R. B.; Ringnalda, M. N.; Sitkoff, D.; Honig, B. *J. Phys. Chem.* **1996**, *100*, 11775−11788.
(100) Zawodzinski, T. A.; Springer, T. E.; Davey, J.; Jestel, R.; Lopez, C.; Valerio, J.; Gottesfeld, S. *Electrochim. Acta* **1995**, *40*, 297−302.
(101) Okada, T.; Xie, G.; Meeg, M. *Electrochim. Acta* **1998**, *14*, 2141−2155.